LANGMUIR

pubs.acs.org/Langmuir Article

Indocyanine Green Assembled Nanobubbles with Enhanced Fluorescence and Photostability

Li Yang, Bin Huang, Feng Chen, Juan Jin, Zhiguo Qin, Fang Yang,*,‖ Yan Li, and Ning Gu*,‖

Cite This: *Langmuir* 2020, 36, 12983−12989 Read Online

ACCESS | Metrics & More | Article Recommendations

Downloaded via SOUTHEAST UNIV on March 18, 2021 at 09:05:45 (UTC).
See https://pubs.acs.org/sharingguidelines for options on how to legitimately share published articles.

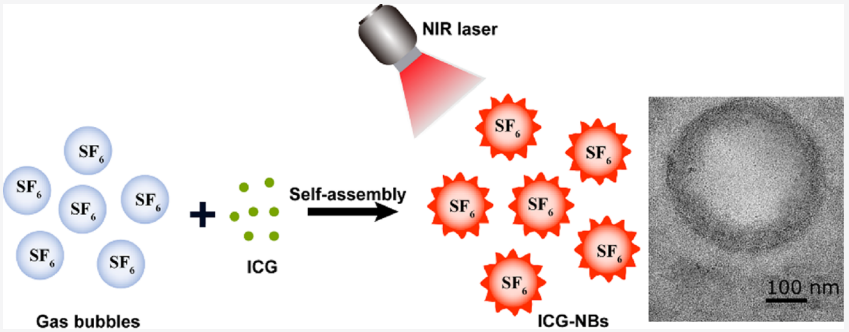

ABSTRACT: Indocyanine green (ICG) is a near-infrared (NIR) fluorescent dye for extensive biomedical application. However, its fluorescence intensity is limited by its poor aqueous stability and concentration-dependent aggregation. To overcome these limitations, ICG self-assembled nanobubbles (ICG-NBs) with an average size of 244.6 nm are fabricated. In the ICG-NB assembled structures, the ICG molecules are arrayed on the gas−liquid interface by the hydrophobic interaction with the gas core and hydrophilic heads with water. Results show that ICG-NBs exhibited good monodispersity and excellent fluorescence and size stability. Compared with ICG solution, the ICG-NBs indicate the enhanced quantum yield and fluorescence intensity. The surface-enhanced Raman scattering (SERS) spectra and fluorescence lifetime measurement demonstrate that the ICG molecule assembled NBs could result in the changes of molecular vibration and time-resolved intensity decays of ICG. Thus, the ICG-NBs could be more beneficial for optical imaging in clinical applications in the future.

INTRODUCTION

Indocyanine green (ICG), a near-infrared (NIR) fluorescent agent approved by the U.S. Food and Drug Administration (FDA) for human use,[1,2] has shown great potentials in fluorescence imaging and photodynamic therapy because of its unique photomechanical, photochemical, and photobiological properties.[3] Unfortunately, ICG possesses some drawbacks such as poor aqueous stability and concentration-dependent aggregation, which limits its application in clinics.[4−6] Enormous efforts have been performed to overcome these limitations. For instance, ICG is encapsulated by protein, membrane, or micelle systems to decrease the aggregation.[7−9] In order to improve the stability, ICG is loaded into polymers to fabricate nanoparticles[10−12] or nanoparticle-assembled capsules.[5,13,14] However, compared with free ICG, all these ICG-based nanostructures exhibit equivalent or lower fluorescence intensity. Furthermore, the added components other than ICG may increase biological toxicity and reduce the biocompatibility. Therefore, there is an urgent need to develop a simple method to overcome the disadvantages of ICG.

Nanobubbles (NBs) are nanoscopic gaseous (typically air) cavities in aqueous solution that have the ability to change the normal behavior and characteristics of the solution. For example, NBs display an enhanced permeability and retention effect in vivo to be retained in the tumor area for a long time.[15] The NBs can also serve as contrast-enhanced agents for ultrasonic imaging.[15] In addition, the NBs have the ability to passively target tumors and show potential for drug/gene delivery to tumors.[16] However, there is no report on how NBs are related to the fluorescence intensity of ICG aqueous solution.

Inspired by the intrinsic properties of NBs, we tuned our attention to combine NBs with free ICG. In this contribution, ICG is directly self-assembled with sulfur hexafluoride (SF_6)-based NBs to fabricate ICG-NBs. It is demonstrated that ICG-NBs exhibit enhanced fluorescence intensity and stability compared with free ICG at the same concentration. The

Received: August 4, 2020
Revised: October 7, 2020
Published: October 21, 2020

ACS Publications © 2020 American Chemical Society

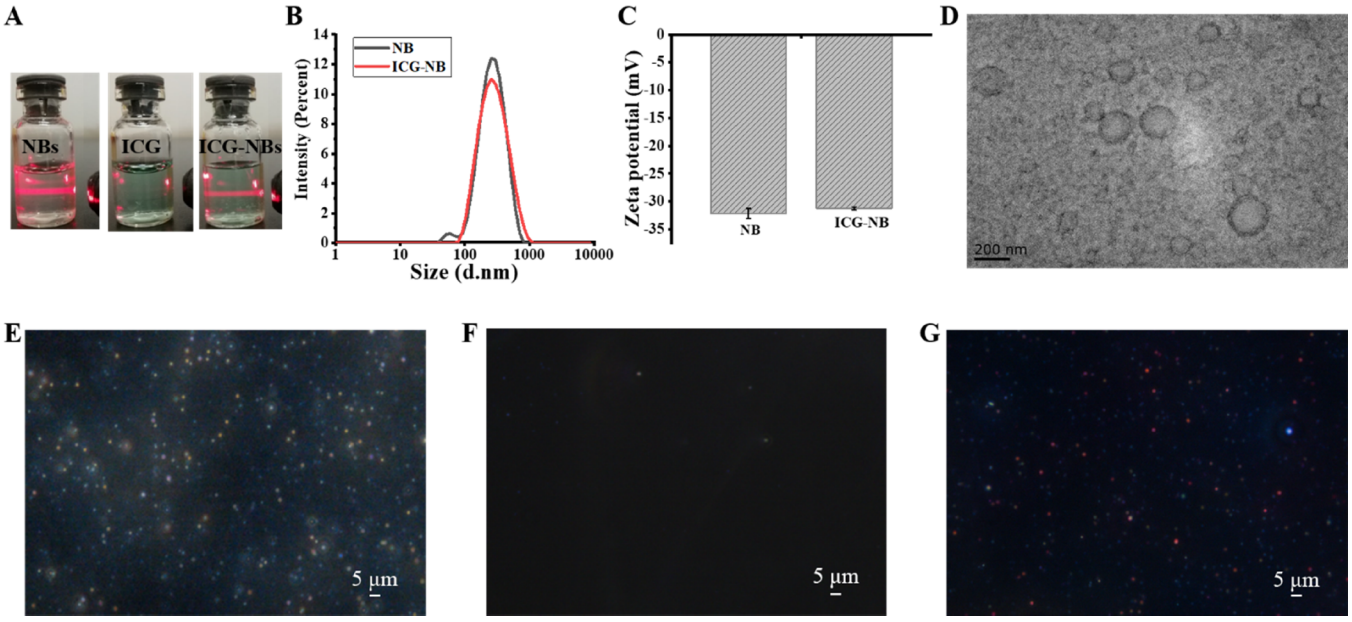

Figure 1. Characterization of the ICG-NBs with a concentration of 10 μg/mL: (A) Tyndall phenomenon of NB, ICG, and ICG-NB solutions; (B) intensity distribution of the NBs and ICG-NBs in the solutions; (C) average zeta potential of NBs and ICG-NBs in the solutions; (D) TEM image of the ICG-NBs; DFM images of NBs (E), free ICG (F), and ICG-NBs (G) in the solutions (scale bar, 5 μm).

hydrodynamic diameter of ICG-NBs was characterized by dynamic light scattering (DLS) measurement, and morphology was visualized and distinguished from free NBs with dark-field microscopy (DFM) and transmission electron microscopy (TEM). The fluorescence property and photostability of ICG-NBs in aqueous media were evaluated by NIR fluorescence imaging and fluorescence spectroscopy, respectively. The self-assembled NB resulted in the change of molecular vibration of ICG and was characterized by SERS spectra. Furthermore, time-resolved intensity decays were measured to demonstrate the photostability of ICG-NBs.

EXPERIMENTAL SECTION

Materials. In our study, ultrapure water with a resistivity of 18.25 MΩ. cm was prepared with a purification system (Youpu Ultrapure Technology Co., Ltd., P. R. China). The ultrapure water was used to generate nanobubbles and dissolve the ICG. ICG for injection was purchased from Dandong Yichuang Pharmaceutical Co., Ltd. (Dandong, China). SF_6 with a purity of 99.99% was purchased from Anhui Qiangyuan Gas Co., Ltd. (Wuhu, China).

Preparation of the ICG-NBs. The NBs with average diameter about 240 nm were fabricated according to the repeated compression method reported in the literature.[17,18] In a typical procedure, after being filled with 2 mL of ultrapure water and oversaturated SF_6, the vial bottle was connected to a medical syringe filled with 3 mL of SF_6 gas. The NBs were generated in the vial bottle by changing the inside pressure periodically. ICG was dissolved in ultrapure water at concentrations of 50, 100, and 200 μg/mL at room temperature. Followed by adjusting the volume ratio of free NBs/free ICG/ultrapure water to 1:1:8 (R1), 5:1:4 (R2), and 9:1:0 (R3), ICG-NB samples with final ICG concentrations of 5, 10, and 20 μg/mL were prepared. When the ICG concentration is above 5 μg/mL, the fluorescence intensity of ICG decreases with the increasing ICG concentration. So, above 5 μg/mL is considered to be a high concentration in this research. Then, ICG concentration was diluted to 2 μg/mL to prepare the low concentration as ICG-NBs′. By adjusting the volume ratio of free NBs/free ICG/ultrapure water to 0.31:1:8.69 (R1′), 0.47:1:8.53 (R2′), 0.63:1:8.37 (R3′), 0.78:1:8.22 (R4′), 0.92:1:8.08 (R5′), 1.09:1:7.91 (R6′), 1.25:1:7.75 (R7′), 1.41:1:7.59 (R8′), and 1.56:1:1.44 (R9′), nine samples of ICG-NBs′ with a final ICG concentration of 0.2 μg/mL were prepared.

DLS Measurement and Morphology. The size and zeta potential of ICG-NBs were measured by using a Zetasizer Nano ZS90 (Malvern, U.K.) instrument equipped with a 532 nm laser at a scattering angle of 90°. The refractive index of the material was set to 1.0 corresponding to air. The morphology and particle size of ICG-NBs were obtained using TEM (JEM-2100, JEOL Ltd., Japan). DFM was used to observe the structure of the ICG-NBs in the solution. The freshly prepared ICG-NBs were taken out with a pipette and dropped on the clean glass slide then covered with a borosilicate coverslip. The sample was observed by DMF at room temperature. The white collimated LED lamp source (TI2-D-LHLED, Japan) focused through a dark-field condenser (NA 0.95−0.80) was used to illuminate the ICG-NB dispersion. The scattering signals of ICG-NBs was collected by a 40× objective and imaged with a CCD camera.

Spectroscopic Measurements and Fluorescence Stability. On consideration of the detection limit of fluorescence spectroscopy, the fluorescence properties of NBs assembled with high concentration of ICG were investigated with NIR fluorescence imaging. NIR fluorescence imaging was performed using an ex/in vivo imaging system (IVIS Spectrum, PerkinElmer, USA). The free ICG, ICG-NBs-R1, ICG-NBs-R2, and ICG-NBs-R3 with ICG concentrations of 5, 10, and 20 μg/mL (twelve samples in total) were transferred into the 12-well plate for NIR fluorescence imaging at an excitation wavelength of 780 nm. The fluorescence intensities of ICG and ICG-NB solutions were further quantitatively analyzed with the NIR fluorescence images. The fluorescence properties of NBs assembled with low concentration of ICG were investigated with fluorescence spectra. The fluorescence spectra were characterized with fluorescence spectroscopy (FluoroMax-4, HORIBA Jobin Yvon, Ltd., France). The fluorescence intensity of ICG-NBs and free ICG was tested at an excitation wavelength of 764 nm.

Calculation of Fluorescence Quantum Yield (Φ_F). The ICG concentrations of ICG-NBs and free ICG were adjusted to 10 μg/mL for calculation of Φ_F. The absorption spectra of samples were recorded on a UV−VIS−NIR spectrophotometer (UV-3600, Shimadzu, Japan). The Φ_F of the ICG-NBs was compared to the free ICG based on the results of absorption and fluorescence spectra. The Φ_F of ICG-NBs was determined with a relativistic approach described by Williams et al.[19] This method involves the use of a well-

https://dx.doi.org/10.1021/acs.langmuir.0c02288
Langmuir 2020, 36, 12983−12989

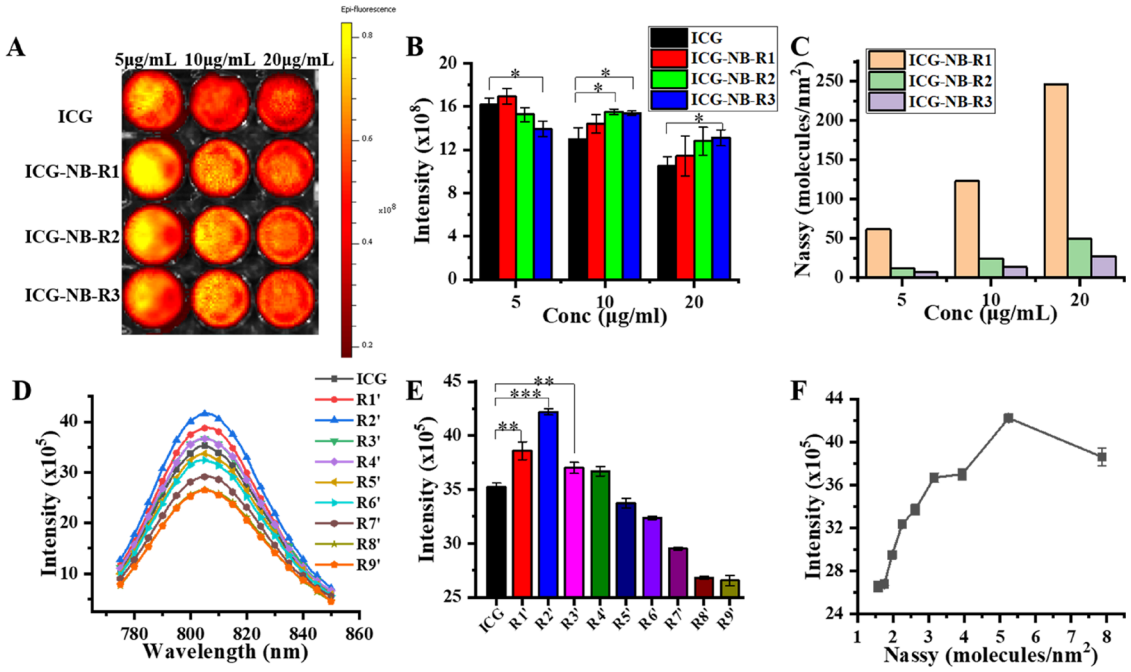

Figure 2. Fluorescence property of ICG-NBs with high and low concentration of ICG: (A) NIR fluorescence images of ICG-NBs with high concentration of ICG and different NB volume ratios and (B) corresponding statistical results of fluorescence intensity measured in (A) (∗ indicated $P < 0.05$); (C) Nassy for ICG-NBs with high concentration of ICG; (D) fluorescence spectrum of ICG-NBs′ with low concentration of ICG (0.2 μg/mL) and different NB volume ratios and (E) corresponding statistical results of fluorescence intensity peaks (∗∗ indicated $P < 0.01$ and ∗∗∗ indicated $P < 0.001$); (F) relationships between Nassy for ICG-NBs′ with low concentration of ICG and fluorescence intensity.

characterized reference molecule of known fluorescence quantum yield, and the overlap of absorption and emission spectra of test and reference molecules. The expression defining the relative Φ_F is given as eq 1

$$\Phi_F = \Phi_{Fref}\left(\frac{\eta^2}{\eta_{ref}^2}\right)\left(\frac{I}{A}\right)/\left(\frac{I_{ref}}{A_{ref}}\right) \quad (1)$$

Where, the Φ_F and Φ_{Fref} are fluorescence quantum yields of test samples (ICG-NBs in water) and reference samples (free ICG in water), respectively; I/A and I_{ref}/A_{ref} are the slopes of fluorescence integrated intensity versus absorption for test and reference samples, respectively; η and η_{ref} are the respective values of the refractive index for the test and reference solvent/suspension media. The Φ_F of the ICG-NBs or free ICG in aqueous solution is determined by comparison with a standard (freshly prepared ICG solution in ultrapure water, Φ_{Fref} = 1.6%).[20]

Fluorescence Lifetime and SERS Spectral Measurements. The fluorescence lifetime and SERS spectra were measured to obtain the structural characteristics of ICG molecules when arranged on the surface of NB. Time-resolved photoluminescence was recorded on an Edinburgh Analytical instrument FLS920 (Edinburgh Instruments, Ltd., England). The SERS spectra of ICG-NB in gold colloidal solution were characterized by a Raman spectrometer (RENISHAW, England) equipped with a 780 nm laser beam. The laser was focused on the sample through a 50× long working distance objective lens. The same microscope objective was also used to collect Raman scattered light.

RESULTS AND DISCUSSION

Characterization of ICG-NBs. The NBs were first fabricated by using the repeated compression method.[17] Next, the free ICG solution was added to freshly prepared NBs to produce ICG-NB solution. First, in order to demonstrate the presence of NBs in solutions, the Tyndall phenomenon was observed by utilizing a laser beam (Figure 1A). The prepared ICG, NB, and ICG-NB solutions were transferred into the vial bottles. A laser pointer (Beijing Whist Science and Technology Development Center, P. R. China) was used to irradiate the sample in the vial bottle. As expected, there was no light path in the free ICG solution. In sharp contrast, obvious light paths were observed in both NB and ICG-NB solutions, indicating the colloid nature of both solutions.

To evaluate the hydrodynamic particle size and zeta potential of the ICG-NBs and NBs in the solutions, DLS measurements were performed at room temperature. The average values of the size and zeta potential of NBs and ICG-NBs were obtained with the arithmetically calculated values by a triplicate experiment. As shown in Figure 1B, the size distribution of NBs was from 50 to 700 nm, while that of ICG-NBs was from 80 to 1100 nm. The average sizes of NBs and ICG-NBs were 237 and 244.6 nm with polydispersity indices of 0.18 and 0.19, respectively, which demonstrates the self-assembly of NBs and ICG. Additionally, the average zeta potentials of NBs and ICG-NBs were estimated to be −32.2 and −31.2 mV, respectively (Figure 1C). The NBs and ICG-NBs showed similar negative zeta potential, reflecting their high colloidal stability in the solutions. The results of a TEM image (Figure 1D) demonstrated that the ICG molecules assembled on the NBs and formed the shell of ICG-NBs. The result of size measured by TEM has shown the consistency with the DLS measurements.

Moreover, DMF was applied to characterize the existence of NBs and ICG-NBs. The DFM images of NB, free ICG, and ICG-NB solutions are shown in Figure 1E−G. It was seen that the DFM image of free ICG solution (Figure 1F) emitted dim light, which can be attributed to its homogeneous phase nature. In contrast, the DFM images of NB and ICG-NB solutions presented lots of light spots (Figure 1E and G),

https://dx.doi.org/10.1021/acs.langmuir.0c02288
Langmuir 2020, 36, 12983−12989

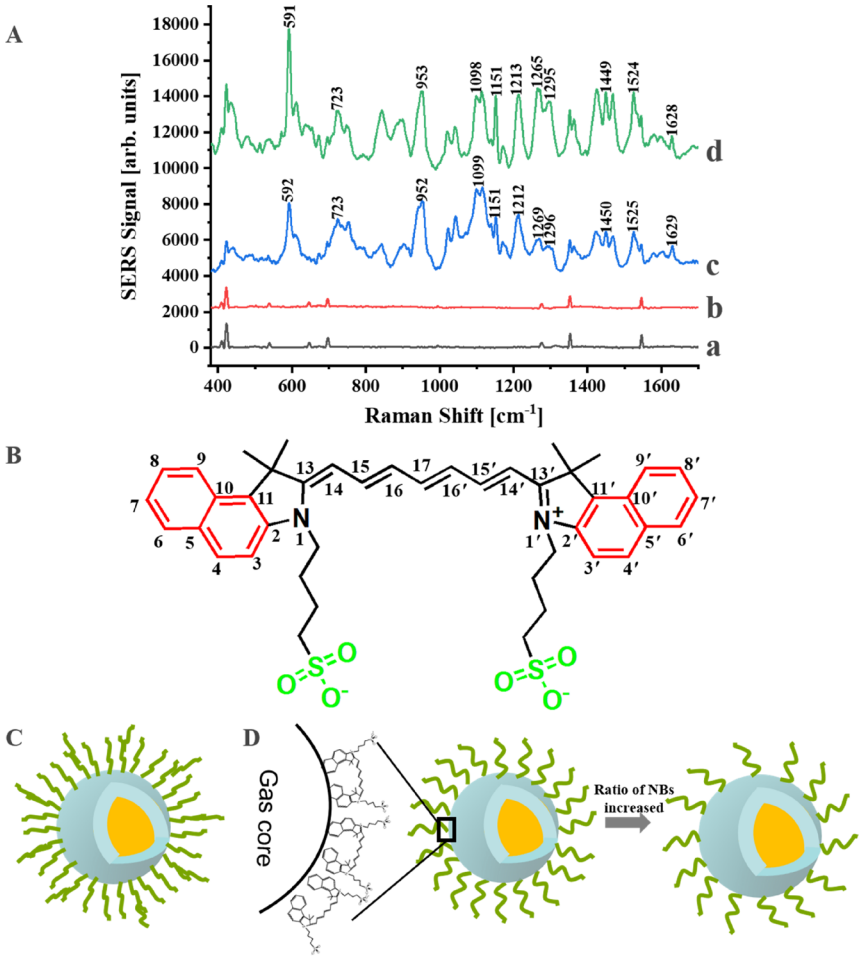

Figure 3. SERS spectra measured from (A) Au (a), NBs (b), free ICG (c), and ICG-NB (d) in gold colloidal solutions. All the spectra were normalized at ca. 952 cm^{-1}, and baseline corrections were performed. All the measurements were carried out at λ_{exc} = 784 nm. (B) Molecular structure and atom numbering of an ICG molecule. (C) Possible structure of ICG-NBs with high concentration of ICG. (D) ICG-NBs′ with low concentration of ICG and an optimal to excess volume ratio of free NBs.

indicating the existence of NBs in both solutions. However, the light spots of DFM images exhibited purple and spherical ICG-NBs due to the ICG molecules bound to the surface of NBs, suggesting that the free ICG molecules were self-assembled with NBs in the solution.

Fluorescence Properties. Three samples of ICG-NB (ICG-NBs-R1, ICG-NBs-R2, and ICG-NBs-R3) solutions with various ICG concentrations of 5, 10, and 20 μg/mL were prepared according to the method mentioned in the Experimental Section. The fluorescence images of the solutions were obtained using an ex/in vivo imaging system. First, each sample with 3 mL was dropped into the 12-well plate. After being filled with these twelve samples, the 12-well plate was placed into the imaging chamber for NIR fluorescence imaging. Six photographs were taken for each well in quick succession and averaged to be one picture. As shown in Figure 2A, the fluorescence decreased with the increase in ICG concentration, which can be attributed to the fluorescence self-quenching of ICG at high concentration. Meanwhile, under the same concentration, compared with the free ICG solution, the fluorescence of ICG-NB solutions was enhanced. The results indicated that after being assembled with nanobubble structure, the self-quenching of ICG in solutions could be avoided.

To investigate the enhancement effect of assembly of free ICG molecules and NBs on fluorescence, the fluorescence intensities of ICG-NB solution were characterized and are shown in Figure 2B. At high ICG concentrations of 10 and 20 μg/mL, with the increase in the ratio of NBs, the fluorescence intensity of solutions increased. Statistical analysis indicates that there is a significant difference between the fluorescence intensities of ICG-NB and ICG solutions. Compared with the corresponding free ICG solution, the maximal fluorescence intensities of ICG-NBs-R2 and ICG-NBs-R3 increased by 19.6 and 25.0%, respectively. In the case of an ICG concentration of 5 μg/mL, the fluorescence intensity of ICG-NBs first increased and then decreased with the increasing ratio of NBs. Furthermore, by adjusting the ICG concentration to 10 μg/mL, the Φ_F of free ICG, ICG-NBs-R1, ICG-NBs-R2, and ICG-NBs-R3 was studied. Freshly prepared ICG solution in ultrapure water was used as a standard. The measured Φ_{Fref} was 0.016. The Φ_F of ICG-NBs-R1, ICG-NBs-R2, and ICG-NBs-R3 were 0.0165, 0.0191, and 0.0189, respectively. With the enhanced fluorescence intensity and smaller absorbance, the ICG-NBs-R2 displayed the largest Φ_F. The number of ICG molecules assembled on the bubble has been investigated more accurately to reveal the effect of NBs on the fluorescence enhancement.

https://dx.doi.org/10.1021/acs.langmuir.0c02288
Langmuir 2020, 36, 12983−12989

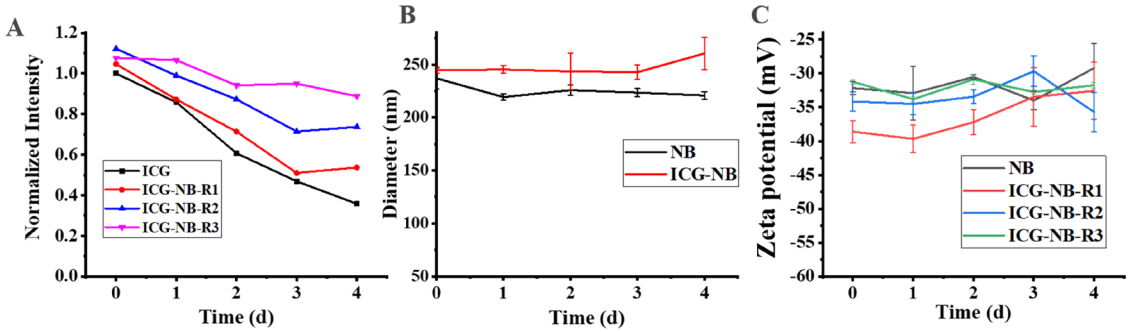

Figure 4. Aqueous stability: (A) ICG fluorescence stability of the ICG-NBs (the fluorescence stability of ICG was significantly improved by self-assembly with NBs); (B) size stability of the ICG-NBs and NBs; (C) zeta potential stability of the ICG-NBs and NBs.

The number of ICG molecules per square nanometer assembled on the bubble (defined as ICG molecule assembly density, Nassy) can be worked out according to the concentration of freshly prepared NB solution (3.49×10^9 NBs/mL), the ICG concentration, and the added volume ratio of free NBs and free ICG. The Nassy for ICG-NBs-R1, ICG-NBs-R2, and ICG-NBs-R3 solutions with various ICG concentrations of 5, 10, and 20 μg/mL is displayed in Figure 2C. When the ICG concentration is 10 μg/mL, the Nassy values are 123, 25, and 14 ICG/nm^2 for ICG-NB-R1, ICG-NB-R2, and ICG-NB-R3, respectively. The result indicates that with the increase in bubble concentration, the fluorescence intensity is increased. Similarly, at an ICG concentration of 20 μg/mL, the Nassy values are 246, 49, and 27 ICG/nm^2 for ICG-NB-R1, ICG-NB-R2, andICG-NB-R3, respectively. Also, the fluorescence intensity is enhanced with the increase in bubble concentration. In particular, the largest enhancement for ICG-NB with ICG concentrations of 10 and 20 μg/mL occurred at Nassy of 25 and 27 ICG/nm^2, respectively. However, when the ICG concentrations is 5 μg/mL, the fluorescence intensity of ICG-NB at a Nassy of 62 ICG/nm^2 has been enhanced, while at 12 and 7 ICG/nm^2, it has been suppressed.

As shown in the above results, to increase the fluorescence intensity, the Nassy of ICG-NBs should be greater than 12 ICG/nm^2. Continuing to increase Nassy to 25 ICG/nm^2, the fluorescence intensity can be enhanced to maximum. Therefore, the ICG and NB self-assembly strategy could probably be a potential way to reduce the use dosage of ICG and enhance fluorescence intensity. The results also suggest that the ratio of NBs might have a significant effect on efficacy of fluorescence enhancement. In order to obtain enhanced fluorescence intensity, it should be optimized in the case of low concentration of ICG solution.

Next, we systematically investigated the influences of different ratios of NBs on the fluorescence intensities of ICG-NBs′ with low concentration of ICG solution (0.2 μg/mL). The fluorescence spectra of ICG-NBs′-R1′, ICG-NBs′-R2′, ICG-NBs′-R3′, ICG-NBs′-R4′, ICG-NBs′-R5′, ICG-NBs′-R6′, ICG-NBs′-R7′, ICG-NBs′-R8′, ICG-NBs′-R9′, and free ICG solutions are shown in Figure 2D. For concise display, they are represented as R1′ to R9′. The fluorescence emission peaks of ICG-NBs′-R1′ to R9′ are almost the same, indicating that the ratio of NBs has negligible influences on the fluorescence spectrum of ICG-NB solutions. However, it was found that the ratio of NBs played an important role on the fluorescence intensity of ICG-NB′ solution. Statistical analysis shown in Figure 2E indicates the significant difference between the ICG-NB′ and free ICG solutions. Among all ICG-NB′ samples, ICG-NBs′-R2′ solution exhibited a 1.20-fold fluorescence intensity enhancement compared to free ICG solution. Based on the concentration of freshly prepared NB solution (3.49×10^9 NBs/mL), the added volume ratio of free NBs and free ICG, and the ICG concentration, Nassy for ICG-NB′ can also be calculated. The relationships between Nassy and fluorescence intensity is plotted in Figure 2F. The fluorescence intensity first increased and then decreased with the increased Nassy. By adding an optimal volume ratio of free NBs (about 1.64×10^8 NBs/mL), the ICG-NBs′-R2′ solution contained 1.55×10^{14} ICG molecules per milliliter. About 5 ICG/nm^2 assembled on the bubble, the fluorescence intensity of ICG-NBs′ at an ICG concentration of 0.2 μg/mL can reach the largest enhancement. The self-aggregation of ICG has been reduced in low concentration solution. Therefore, smaller Nassy for ICG-NBs′ can also enhance the fluorescence intensity compared to the ICG-NBs.

SERS Spectral Measurement. To better understand the molecular changes, we measured SERS spectra of free ICG and ICG-NB in gold colloidal solution by a RENISHAW Raman spectrometer (Figure 3A). The molecular structure and part of atom numbering of an ICG molecule are shown in Figure 3B. Both spectra of ICG and ICG-NB show very similar SERS features. However, a control sample, consisting of NBs complexed with gold nanoparticles, did not produce SERS signals, which shows almost the same SERS features as gold nanoparticles. Comparing the spectra in Figure 3A, the ICG-NBs exhibit a stronger SERS spectrum than free ICG solution. The reason may be that the SERS intensity is associated with molecular aggregation in free ICG solution.[21] Specially, a marked increase in relative intensity is observed for the band at 1151 cm^{-1}, attributed to ν(phenyl ring) and δ(CH) contributions (ν, stretching; δ, deformation). Compared with free ICG (at 1269 cm^{-1}), the ICG-NB demonstrates a stronger SERS spectrum and a slight blueshift at 1265 cm^{-1}, attributed to δ(CH) of the C13C13′ and δ(C15,15′-H) contributions. The ICG-NB also exhibits intensity increase at 1295 cm^{-1}, attributed to δ(CH) of the C13C13′ and δ(C15,15′-H). These obvious differences of SERS spectra between the ICG-NB and ICG may be due to the assembly of ICG with NB.

According to the results above, we concluded the possible structure of ICG-NBs with high concentration of ICG shown in Figure 3C. The free vibration of an ICG molecule was restricted by high concentration (above 5 μg/mL) of ICG coated on NB. There was more energy consumed by fluorescence radiation.[22] From an optimal volume ratio of free NBs to excess free NBs, the possible structure of ICG-

https://dx.doi.org/10.1021/acs.langmuir.0c02288
Langmuir 2020, 36, 12983−12989

NBs′ at low concentration (with 0.2 μg/mL) of ICG is shown in Figure 3D. The ICG molecules are arrayed on the gas−liquid interface by the hydrophobic interaction with the gas core and hydrophilic heads with water shown as the partially enlarged drawing. The low concentration of ICG assembled with an optimal and excess volume ratio of free NBs is concluded. The optimal volume ratio of free NBs corresponding to optimum Nassy can enhance but the excess volume ratio of free NBs with small Nassy can suppress fluorescence intensity of ICG-NBs′.

Aqueous Stability. By adjusting the ICG concentration to 10 μg/mL, the aqueous stability of ICG-NBs has been studied. Compared with free ICG, the fluorescence spectra of ICG-NBs with different volume ratios of free NBs were demonstrated (Figure 4A). All the spectra were normalized by the first day of free ICG fluorescence intensity, which demonstrated that the ICG assembled with NBs can enhance the fluorescence intensity of ICG. After 1 day, the fluorescence intensity of the ICG-NBs-R3 in ultrapure water remained at ∼99.0%, while the fluorescence intensity of free ICG solution degraded to 85.8%. Figure 4A also shows that the fluorescence intensity of free ICG in ultrapure water was decreased to 35.8% of the initial intensity within 4 days, but the ICG fluorescence intensity of the ICG-NBs-R3 in ultrapure water remained above 82.4%. The ICG self-assembled with NBs significantly enhanced the fluorescence stability of ICG. ICG-NBs showed a better photostability than the reported 72%.[23]

A size and zeta potential stability assay of the ICG-NBs in ultrapure water compared with NBs was performed for 4 days when stored at 4 °C (Figure 4 B and C). The size of ICG-NBs and NBs in ultrapure water kept a similar size for 4 days, suggesting a great long-term stability of the ICG-NBs and NBs. The zeta potential maintained around −35 mV over the test period, also presenting their excellent aqueous stability.

Fluorescence Lifetime. The fluorescence lifetime was determined by measuring time-resolved intensity decays. The intensity decays were analyzed in terms of the exponential model, and fluorescence emitted will decay with time according to eq 2

$$I(t) = I_0 \times \exp(-t/\tau_{\text{delayed}}) \quad (2)$$

Where, t is time, τ_{delayed} is the fluorescence lifetime, and I_0 is the initial fluorescence at $t = 0$. The fluorescence lifetime for free ICG and ICG-NBs were 0.463 and 0.401 ns, respectively (Figure 5). The lifetime of ICG-NBs was shorter as compared to the free ICG solution. It is known that the decreased lifetimes would result in an increased photostability because a shortened lifetime allows less time in the excited state per excitation de-excitation cycle.[24,25]

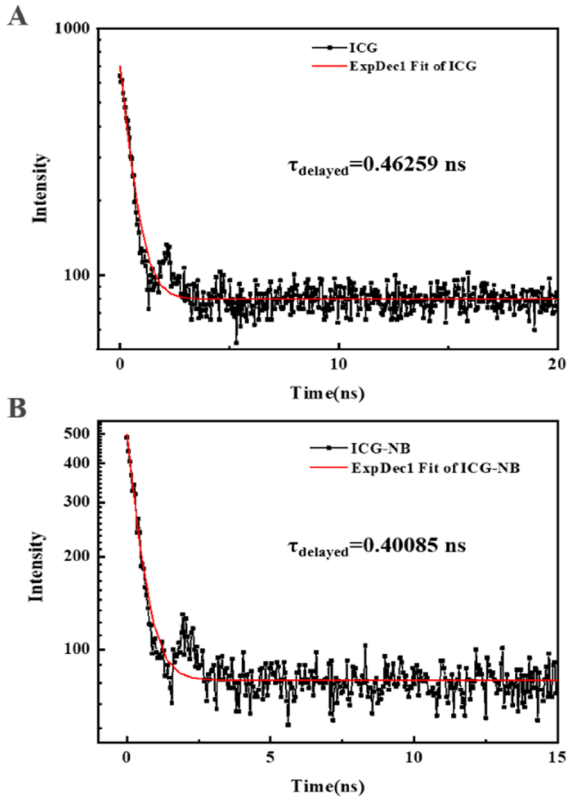

Figure 5. Time-dependent intensity decays of (A) free ICG and (B) ICG-NBs.

CONCLUSIONS

In conclusion, we have demonstrated a self-assembly strategy to enhance the fluorescence and photostability of ICG. The ICG-NBs with high concentration of ICG (above 5 μg/mL) show good fluorescence enhancement compared to free ICG. The molecular vibration was weakened when the high concentration of ICG assembled with NBs. There was more energy consumed by fluorescence radiation. The optimum Nassy was about 25 ICG/nm^2, and the fluorescence intensity can be enhanced to maximum. Upon optimizing the ratios of ICG solution and NBs at a lower ICG concentration of 0.2 μg/mL, the fabricated ICG-NBs exhibited a 1.20-fold fluorescence intensity enhancement compared to free ICG solution. The corresponding Nassy is estimated to be about 5 ICG molecules per square nanometer assembled on the bubble. Furthermore, the ICG-NBs displayed excellent light stability. After 4 days, free ICG in ultrapure water was decreased to 35.8% of the initial intensity, but the ICG fluorescence intensity of the ICG-NBs-R3 in ultrapure water remained above 82.4%. The findings of this research may provide a simple approach to increase photostability and to reduce concentration quenching of ICG in solutions. This self-assembly strategy could probably be a potential way to improve light stability, enhance fluorescence performance, and reduce the use dosage of ICG in clinical applications.

AUTHOR INFORMATION

Corresponding Authors

Fang Yang − *State Key Laboratory of Bioelectronics, Jiangsu Key Laboratory for Biomaterials and Devices, School of Biological Science and Medical Engineering, Southeast University, Nanjing 210096, People's Republic of China;* orcid.org/0000-0001-6922-6348; Email: yangfang2080@seu.edu.cn

Ning Gu − *State Key Laboratory of Bioelectronics, Jiangsu Key Laboratory for Biomaterials and Devices, School of Biological Science and Medical Engineering, Southeast University, Nanjing 210096, People's Republic of China;* orcid.org/0000-0003-0047-337X; Email: guning@seu.edu.cn

Authors

Li Yang − *State Key Laboratory of Bioelectronics, Jiangsu Key Laboratory for Biomaterials and Devices, School of Biological Science and Medical Engineering, Southeast University, Nanjing 210096, People's Republic of China*

https://dx.doi.org/10.1021/acs.langmuir.0c02288
Langmuir 2020, 36, 12983−12989

Bin Huang − *Jiangsu Second Normal University, Nanjing 210013, People's Republic of China*
Feng Chen − *School of Biomedical Engineering and Informatics, Nanjing Medical University, Nanjing 211166, People's Republic of China*
Juan Jin − *State Key Laboratory of Bioelectronics, Jiangsu Key Laboratory for Biomaterials and Devices, School of Biological Science and Medical Engineering, Southeast University, Nanjing 210096, People's Republic of China*
Zhiguo Qin − *State Key Laboratory of Bioelectronics, Jiangsu Key Laboratory for Biomaterials and Devices, School of Biological Science and Medical Engineering, Southeast University, Nanjing 210096, People's Republic of China*
Yan Li − *State Key Laboratory of Bioelectronics, Jiangsu Key Laboratory for Biomaterials and Devices, School of Biological Science and Medical Engineering, Southeast University, Nanjing 210096, People's Republic of China*

Complete contact information is available at: https://pubs.acs.org/10.1021/acs.langmuir.0c02288

Author Contributions

‖F.Y. and N.G. contributed equally.

Notes

The authors declare no competing financial interest.

■ ACKNOWLEDGMENTS

This investigation was financially funded by the project of the National Key Research and Development Program of China (2017YFA0104302) and the National Natural Science Foundation of China (51832001, 61821002, and 81971750). The authors also would like to thank the support from the Collaborative Innovation Center of Suzhou Nano Science and Technology.

■ REFERENCES

(1) Zheng, C.; Zheng, M.; Gong, P.; Jia, D.; Zhang, P.; Shi, B.; Sheng, Z.; Ma, Y.; Cai, L. Indocyanine Green-Loaded Biodegradable Tumor Targeting Nanoprobes for *in Vitro* and *in Vivo* Imaging. *Biomaterials* **2012**, *33*, 5603−5609.
(2) Li, J.; Jiang, H.; Yu, Z.; Xia, H.; Zou, G.; Zhang, Q.; Yu, Y. Multifunctional Uniform Core-Shell Fe_3o_4@$Msio_2$ Mesoporous Nanoparticles for Bimodal Imaging and Photothermal Therapy. *Chem. − Asian J.* **2013**, *8*, 385−391.
(3) Zheng, X.; Zhou, F. Noncovalent Functionalization of Single-Walled Carbon Nanotubes by Indocyanine Green: Potential Nanocomplexes for Photothermal Therapy. *J. X-ray Sci. Technol.* **2011**, *19*, 275−284.
(4) Zheng, X.; Zhou, F.; Wu, B.; Chen, W. R.; Xing, D. Enhanced Tumor Treatment Using Biofunctional Indocyanine Green-Containing Nanostructure by Intratumoral or Intravenous Injection. *Mol. Pharmaceutics* **2012**, *9*, 514−522.
(5) Yaseen, M. A.; Yu, J.; Wong, M. S.; Anvari, B. Laser-Induced Heating of Dextran-Coated Mesocapsules Containing Indocyanine Green. *Biotechnol. Prog.* **2007**, *23*, 1431−1440.
(6) Kirchherr, A.-K.; Briel, A.; Mäder, K. Stabilization of Indocyanine Green by Encapsulation within Micellar Systems. *Mol. Pharmaceutics* **2009**, *6*, 480−491.
(7) Rajagopalan, R.; Uetrecht, P.; Bugaj, J. E.; Achilefu, S. A.; Dorshow, R. B. Stabilization of the Optical Tracer Agent Indocyanine Green Using Noncovalent Interactions. *Photochem. Photobiol.* **2000**, *71*, 347−350.
(8) Rodriguez, V. B.; Henry, S. M.; Hoffman, A. S.; Stayton, P. S.; Li, X.; Pun, S. H. Encapsulation and Stabilization of Indocyanine Green within Poly(Styrene-Alt-Maleic Anhydride) Block-Poly(Styrene) Micelles for near-Infrared Imaging. *J. Biomed. Opt.* **2008**, *13*, No. 014025.
(9) Maarek, J. M. I.; Holschneider, D. P.; Harimoto, J. Fluorescence of Indocyanine Green in Blood: Intensity Dependence on Concentration and Stabilization with Sodium Polyaspartate. *J. Photochem. Photobiol., B* **2001**, *65*, 157−164.
(10) Saxena, V.; Sadoqi, M.; Shao, J. Enhanced Photo-Stability, Thermal-Stability and Aqueous-Stability of Indocyanine Green in Polymeric Nanoparticulate Systems. *J. Photochem. Photobiol., B* **2004**, *74*, 29−38.
(11) Saxena, V.; Sadoqi, M.; Shao, J. Indocyanine Green-Loaded Biodegradable Nanoparticles: Preparation, Physicochemical Characterization and in Vitro Release. *Int. J. Pharm.* **2004**, *278*, 293−301.
(12) Zheng, M.; Yue, C.; Ma, Y.; Gong, P.; Zhao, P.; Zheng, C.; Sheng, Z.; Zhang, P.; Wang, Z.; Cai, L. Single-Step Assembly of Dox/ICG Loaded Lipid-Polymer Nanoparticles for Highly Effective Chemo-Photothermal Combination Therapy. *ACS Nano* **2013**, *7*, 2056−2067.
(13) Yaseen, M. A.; Yu, J.; Wong, M. S.; Anvari, B. Stability Assessment of Indocyanine Green within Dextran-Coated Mesocapsules by Absorbance Spectroscopy. *J. Biomed. Opt.* **2007**, *12*, No. 064031.
(14) Yu, J.; Yaseen, M. A.; Anvari, B.; Wong, M. S. Synthesis of near-Infrared-Absorbing Nanoparticle-Assembled Capsules. *Chem. Mater.* **2007**, *19*, 1277−1284.
(15) Zheng, R.; Yin, T.; Wang, P.; Zheng, B.; Cheng, D.; Zhang, X.; Shuai, X.-T. Nanobubbles for Enhanced Ultrasound Imaging of Tumors. *Int. J. Nanomed.* **2012**, *7*, 895−904.
(16) Duan, L.; Yang, L.; Jin, J.; Yang, F.; Liu, D.; Hu, K.; Wang, Q.; Yue, Y.; Gu, N. Micro/Nano-Bubble-Assisted Ultrasound to Enhance the EPR Effect and Potential Theranostic Applications. *Theranostics* **2020**, *10*, 462−483.
(17) Jin, J.; Feng, Z.; Yang, F.; Gu, N. Bulk Nanobubbles Fabricated by Repeated Compression of Microbubbles. *Langmuir* **2019**, *35*, 4238−4245.
(18) Jin, J.; Wang, R.; Tang, J.; Yang, L.; Feng, Z.; Xu, C.; Yang, F.; Gu, N. Dynamic Tracking of Bulk Nanobubbles from Microbubbles Shrinkage to Collapse. *Colloids Surf., A* **2020**, *589*, 124430.
(19) Williams, A. T. R.; Winfield, S. A.; Miller, J. N. Relative Fluorescence Quantum Yields Using a Computer-Controlled Luminescence Spectrometer. *Analyst* **1983**, *108*, 1067−1071.
(20) Sevick-Muraca, E. M.; Lopez, G.; Reynolds, J. S.; Troy, T. L.; Hutchinson, C. L. Fluorescence and Absorption Contrast Mechanisms for Biomedical Optical Imaging Using Frequency-Domain Techniques. *Photochem. Photobiol.* **1997**, *66*, 55−64.
(21) Kneipp, J.; Kneipp, H.; Rice, W. L.; Kneipp, K. Optical Probes for Biological Applications Based on Surface-Enhanced Raman Scattering from Indocyanine Green on Gold Nanoparticles. *Anal. Chem.* **2005**, *77*, 2381−2385.
(22) Chen, W.; Chen, C.-L.; Zhang, Z.; Chen, Y.-A.; Chao, W.-C.; Su, J.; Tian, H.; Chou, P.-T. Snapshotting the Excited-State Planarization of Chemically Locked *N,N* '-Disubstituted Dihydrodibenzo [*a,C*] Phenazines. *J. Am. Chem. Soc.* **2017**, *139*, 1636−1644.
(23) Zheng, M.; Zhao, P.; Luo, Z.; Gong, P.; Zheng, C.; Zhang, P.; Yue, C.; Gao, D.; Ma, Y.; Cai, L. Robust Icg Theranostic Nanoparticles for Folate Targeted Cancer Imaging and Highly Effective Photothermal Therapy. *ACS Appl. Mater. Interfaces* **2014**, *6*, 6709−6716.
(24) Geddes, C. D.; Parfenov, A.; Roll, D.; Uddin, M. J.; Lakowicz, J. R. Fluorescence Spectral Properties of Indocyanine Green on a Roughened Platinum Electrode: Metal-Enhanced Fluorescence. *J. Fluoresc.* **2003**, *13*, 453−457.
(25) Geddes, C. D.; Cao, H.; Gryczynski, I.; Gryczynski, Z.; Fang, J.; Lakowicz, J. R. Metal-Enhanced Fluorescence (Mef) Due to Silver Colloids on a Planar Surface: Potential Applications of Indocyanine Green to in Vivo Imaging. *J. Phys. Chem. A.* **2003**, *107*, 3443−3449.